Analysis of polarized microwave emission of Flare-Productive Active Region 9415

¹V.M.Bogod, ²G.B.Gelfreikh, ³F.Ch.Drago, ⁴V.P.Maximov, ⁵A.Nindos, ¹T.I.Kaltman, ⁶B.I.Ryabov, ²S.Kh.Tokhchukova

¹Special Astrophysical Observatory, Nizhnij Arkhyz, Russia
²Pulkovo Astronomical Observatory, St.Petersburg, Russia
³Institut of Solar-Terrestrial Physics, Irkutsk, Russia
⁴ Universita degli Studio di Firenzi, Florence, Italy
⁵University of Ioannina, Greece

⁶Ventspills International Radioastronomical Center, Riga, Latvia

Abstract

The results of the microwave observations of the Sun made with the RATAN-600 have shown the existence of many types of spectral peculiarities in polarized emission of active regions, which produce powerful flares. These phenomena happen at microwaves and reflect inhomogeneous structure of magnetic field in magnetospheres of flaring active regions in wide range of heights above the photosphere. In this presentation we demonstrate an analysis of the AR 9415 during all the period of its passage across the solar disk. Results of the study point out to existence of different scenarios of circular polarization variations in the radio wave band. Here, we separated the phenomenon of the cyclotron emission passage through the quasi-transverse magnetic field (QT-region) and several effects connected with flare activity of active region. New observational data are presented and compared with the data of several observatories: SSRT, NoRH, MDI SOHO, GOES and MEES. The preliminary interpretation of the phenomena are given.

^{*}vbog@gao.spb.ru

1 Introduction

The nature of flare-productive active regions (FPAR) on the Sun is enriched by diversity of polarization emission features in wide range of microwaves. It was found from detailed spectral-polarization study that solar active regions demonstrate various polarization peculiarities depending on their flaring activity. The well-known phenomenon of circular polarization inversion due to radio emission passage through quasi-transverse magnetic field region was detected and studied in detaila in papers [19], [16], [11]. The coupling mode theory created in the works [12] and [25] is the physical base for interpretation of this phenomena in observations. Due to the close geometrical binding to spatial height structure of magnetic field (it must be located perpendicularly to the line of sight), it is possible to reconstruct a vertical magnetic field distribution up to several hundred Mm.

From the other side, the dynamic processes going on in active regions frequently complicate the spectral and temporal behavior of QT-effect. Therefore the main aim of this paper is to show the main difference of QT-effect from other polarization phenomena intrinsic to flare processes in AR. As for the AR 9415, evolution of its circular polarization structure was very complicated. Nevertheless, the evolution of polarization inversion due to the QT-phenomenon was recorded clearly both on time and on spectrum. At the same time the observed circular polarization in sunspot associated sources caused by cyclotron emission due to strong magnetic fields, changed greatly up to multiple inversions. It points out to the influence of multi-arch magnetic structure to transmitted polarized microwave emission.

Recently, in the paper [8] it was shown that polarizated microwave emission of FPAR's demonstrate some very peculiar features, mostly in the wavelength range from 2 to 5 cm. Among them, a narrow-band short-wave (normally shorter than 3.5cm) polarization inversion and polarization brightening, designated correspondingly as effects A1 and A2. Also multiple spectral inversions inside of 10-20% of frequency (named as effect B), and a wide band feature of microwave "darkening" of emission intensity [22]. All of these features were registered in the AR 9415 both on the early preparatory stage during several days before the powerful events and on the eruptive stage of flare.

Several features in polarization inversions were detected in early radio observations using the movement of AR along the disc [19]. Additional fine features were found using model idea about geometry of quasi-transverse pas-

sage [20]. In particular, spectral-polarization behavior of sunspot associated source emission during its multiple passage through QT-regions was studied [21]. From the other side, the effects of multiple spectral and temporal polarization inversions intrinsic to FPAR do not have correct interpretation yet. Theoretically, other versions of multiple inversion besides the QT-phenomena are possible. For example, the following mechanisms were considered by several authors: passage of emission through regions with a high turbulence level, with high electron density, and others [10]; inversion due to the change of longitudinal magnetic field sign at the top of coronal arch during the passage of AR along the solar disc [1], [2]; passage of cyclotron emission trough current sheets [14] and passage of region with inverse gradient of temperature with height [24], [15], etc.

2 Observations

2.1 RATAN-600

For the research we have used opportunities of the radiotelescope RATAN-600 (located in Northern Caucasus, Russia), which has optimum parameters for the research of preflare plasma in active regions. For the current task it was the most important the combination of an instant spectrum in a wide frequencies range (1.7cm - 8cm) with a good spectral resolution (5 - 7%), high accuracy of polarization measurements (< 0.05%), and high brightness temperature sensitivity (< 10K). RATAN-600 has a moderate spatial resolution in a horizontal plane (< 15'' at 2cm) and relatively low resolution in a vertical plane (< 15' at 2cm), which varies proportionally to the wavelength. Observations were carried out daily from about 7:00 UT to 11:00 UT with a time cadence of 8 minutes. The obtained one-dimensional images ("scans") of the Sun are published at:http://www.sao.ru/hq/sun/ [9].

2.2 SSRT

Siberian Solar Radio Telescope (SSRT) is a heliograph consisting of 256 antennas and working at the wavelength of 5.2 cm. It obtains two-dimensional radio maps of the sun with spatial resolution about 20" each 3-4 minutes. We have used observations presented in Internet: http://ftp://iszf.irk.ru/pub/ssrt_data/fits/.

2.3 NRH

The 2D observations made with Nobeyama radioheliograph (NRH) at the wavelength 1.76cm with spatial resolution $10'' \times 10''$ in intensity and circular polarization were taken from the site:

ftp://solar.nro.nao.ac.jp/pub/norp/data/daily/. For the comparison with RATAN-600 data the 2D maps were convolved with the RATAN-600 beam at wavelength 1.83cm.

2.4 SOHO MDI and GOES

The satellite data were used for obtaining of information about the flare class (GOES) and magnetic field structure on the photosphere level (SOHO MDI). The magnetograph data of SOHO MDI in FITS format with 96 minute cadence were obtained from the site: http://soi.stanford.edu/magnetic/mag/and GOES data from http://www.sec.noaa.gov. In the necessary cases a convolution with the different wavelength beams of RATAN-600 was performed. Up to now the satellite data are the good base for associating the radio data.

2.5 Mees data

The data of this observatory were used for quick determination of magnetic field configuration of the AR 9415. They were taken from the site http://www.solar.ifa.hawaii.edu/ARMaps/.

3 Total information about the active region AR 9415

Let us consider development of our AR in period from April 3 till April 15 of 2001. Magnetic configuration of the region was rather complicated. According to the data obtained at the observatory Mees, it passed through following stages of development: β (3-4.04), $\beta - \gamma$ (5-7.04), $\beta - \gamma - \delta$ (8-13.04), $\beta - \gamma$ (14.04), and again β (15.04). 69 flares were registered in the region, including 6 X-ray bursts of I level and 5 of O. We have used the RATAN-600 to study spectral polarization structure of the AR and radio maps obtained with the SSRT to get its two-dimensional structure at wavelength of 5.2cm. Space observations from GOES and SOHO MDI were used to get information

on parameters of flares and the structure of the photospheric magnetic fields. The Table 1 summarizes information on evolution AR9415 found from all the above instruments during the period under study.

4 Three periods of evolution of the AR 9415

Three periods of powerful flaring activity one can follow in the AR 9415 using GOES data on Figure 3) and the Table I. The first period was from April 3 to 6, when weak activity of the AR 9415 took place on the ground of powerful activity of the preceding AR 9393. The second period was registered from the April 7 to 14 and the third from 12 to 14. Each period was beginning from low activity and was finished by generation of powerful flares of the level M or X.

It is interesting to note that does not seem any correlation between microwave polarization spectra (observations made with the RATAN-600 and SSRT) and variations in magnetic structure at the photospheric levels (MDI SOHO and Mees data). The latter showed development to more complicated magnetic structure, from β (April 3) to $\beta - \gamma - \delta$ configuration (from April 8 to 13).

4.1 Period April 3-6

At the Figure 1 the comparison of the radio and optical data during April 3 is presented. Figure 1a shows the location of the AR 9415 on SOHO MDI magnetogram (to the left) and 2D map from SSRT at wavelength 5.2cm (to the right). It is worth mentioning a very complicated β configuration of the magnetic field and dominated one sign RH polarized source in the region. On the Figure 1b the scans of the Sun made with the RATAN-600 are shown at several cm wavelengths. At the top it is shown the scans in intensity and below the scan in circular polarization. One can see that the source of AR 9415 at E limb consist of two components A and B. East source A is located on the distance of 40-45'' (it corresponds to the height about 30 thousand km above photosphere) and demonstrates the inversion of circular polarization from short wave to longer. The other more power source B is located near the limb and has the RH polarized emission. On the Figure 1c at the top the spectrum of polarized emission of the Eastern source is shown. This has an inversion of the sign of polarization around the frequency of

Table 1:

Date	MDI SOHO, MEES	GOES	RATAN-600	SSRT
3.04.	β	X1.2(3h57m)	RH, monotonous spectrum	RH,single source
4.04	β	M1.6(10h27m)	RH, monotonous spectrum	Bypolar source RH,W-side,strong LH, E-side, weak
5.04	$\beta - \gamma$	M5.1(17h25m)	RH,short-wave increase	Single,RH, W-side,
6.04	$\beta - \gamma$	X5.6(19h21m)	RH,short-wave increase	Single,LH,center
7.04	$\beta - \gamma$	Stable	LH,short-wave increase	Bypolar, LH, center, strong RH,E-side,weak
8.04	$\beta - \gamma - \delta$	Stable	LH,short-wave increase	LH,center,strong RH,E-side,weak
9.04	, ,	M7.9(15h34m)	No data	LH, center, strong RH,E-side, strong
10.04	$\beta - \gamma - \delta$	X2.3(5h26m)	LH,short-wave increase	LH,center,strong RH,E-side,strong
11.04	. ,	M2.3(13h26m)	LH,short-wave increase	LH,center,weak RH,E-side,strong
12.04	$\beta - \gamma - \delta$	M1.3(10h28m)	LH,short-wave increase	LH,center,weak RH,E-side,strong
13.04	$\beta - \gamma - \delta$	Stable	RLR inversion	Single RH, strong
14.04	$\beta - \gamma$	M1(18h11m)	RLR inversion	Single RH, strong
15.04	β	X14.4(13h50m)	RLR inversion	No data

11 GHz. At the lower figure we see the spectrum of the main source, one typical for a cyclotron sunspot connected emission. One can suppose that the presence of the higher East component with nonthermal spectrum has something to do with high flaring activity of the AR 9415.

On the Figure 2 the comparison of radio and optical data is presented for the April 5 and 6. The magnetic field map (left column - to the top picture for April 5 and the down for April 6) according SOHO MDI demonstrates the stable structure with small changes. On the contrary the radio map at 5.2cm obtained on the SSRT (second column: up for April 5, down one for April 6) shows polarization inversion from the RH to LH. This is probably due to the effect of wave propagation through the region of QT magnetic field.

At the right the RATAN-600 scans at a number of cm wavelength are presented. Let us note that the sign of polarization registered at SSRT at λ =5.2cm (SSRT) agrees with that at λ =4.93cm observed at RATAN-600. However, already at λ =6.06cm the inversion of polarization in QT region takes place. One should also notice the increase of the polarized emission at short waves (2.32cm - 1.92cm). This kind of event is often connected with appearance of new magnetic flux in the existing AR [8].

According to the observations made with GOES (see Figure 3) the level of flare activity of the AR 9415 in this period was not too high and was observed at the background of the preceding more active region AR 9393.

4.2 Spectra and polarization of the AR9415 in the period of April 6 - 7

According to the RATAN-600 observations the sharp inversion of polarization took place in wide wavelength range from 1.83cm to 3.06cm (see Figure 4). The variations in the structure of the magnetic field at the photosphere according to the optical magnetograph of MDI SOHO were also observed but they did not seem so significant. Observations made with the SSRT showed appearance of a new radio source at the East of the AR 9415.

For more detailed comparison of the radio and optical observations the convolution of optical magnetogram with diagram pattern of the RATAN-600 was made for wavelength λ =2.24cm (17" × 15' size). The results are shown on the Figure 5 for several moments of observations on April 6 and 7. At this Figure the central part of optical magnetogram is shown which is

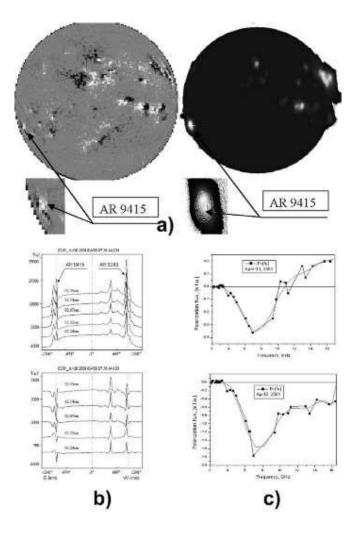


Figure 1: The rising of AR 9415 on the E-limb. a) On the left the solar disc magnetic field map according MDI SOHO data; on the right - the radio map at wavelength 5.2cm made with SSRT, below - the polarized emission map for AR 9415. a)One-dimensional radio scans of AR 9415 made with RATAN-600 during April 3, 2001. Up - the intensity scans at different waves moved in vertical axis. Below-the circular polarization scans (righthanded polarization is negative). AR9415 consist of two radio sources A (above the limb) and B (more intensive). c) The spectra of polarization emission: up for source A, and down - for source B. The smoothed curves with polynomial fit are shown by dotted lines.

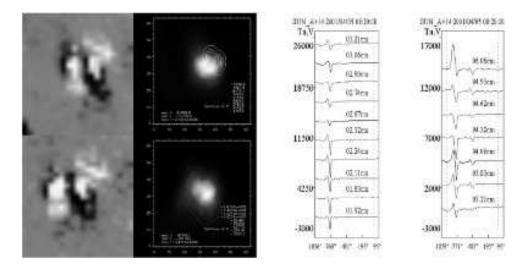


Figure 2: Comparison of photosphere magnetic field data and radio polarization data for AR 9415. On the left - MDI SOHO data, up - MDI map for April 5, down - MDI map for April 6. In the second column: up- the radio map at 5.2cm for April 5, down - the same for April 6. One can see the QT inversion at this wave. To the right, the one-dimensional RATAN-600 polarization emission scans at several wavelengths for April 4, 5 and 6 are presented. One can see the short wave brightening of polarization emission for April 5 and 6. The polarization inversion at longer wavelength 6.06cm is recorded also.

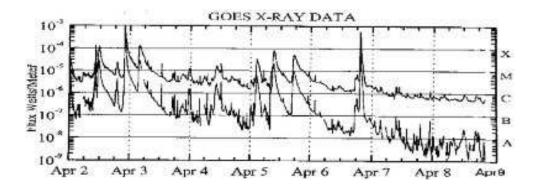


Figure 3: Soft X-ray GOES data during interval from April 2 to April 16, 2001.

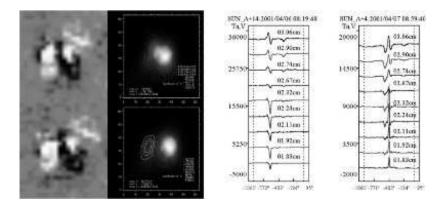


Figure 4: Comparison of photosphere magnetic field data and radio polarization data for AR 9415. On the left - MDI SOHO data, up - MDI map for April 6, down - MDI map for April 7. In the second column: up - the radio map at 5.2cm for April 6, down - the same for April 7. To be note the stable magnetic field structure on the photosphere for both days. To the right, the one-dimensional RATAN-600 polarization emission scans at several wavelengths for April 6 and 7 are presented. One can see the wide band of polarization inversion was occurred between two days.

registered by the RATAN scan of the solar disk. In general one can see that one-dimensional structure of the photospheric magnetic field was stable during these two days period (see Figure 5).

On the Figure 6 the comparison of the radio scans at the wavelength of 2.24cm and integrated to one-dimensional scale magnetograms of MDI SOHO for two times and the two dates, April 6 and 7. One can see that at the radio waves total reversal of the sign of the circular polarization while at the photospheric level no significant variation of the magnetic field structure was registered. The sign of polarization in the radio wave range become correspond to excess of the extraordinary mode. Some oscillations of the optical and radio magnetograms in their related position are also observed in the range of tens of arcsecs. In the time interval between the presented data for the 6 and 7 April a powerful flare happened on (class O5.6) at 19h 21m UT on April 6.

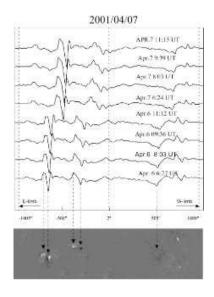


Figure 5: One dimensional magnetic field scans, made in convolution of 2D map of MDI SOHO with one-dimensional RATAN-600 beam. One can see the stability of photosphere magnetic field structure during two days for several time moments. The AR 9415 is located at east part of the disc.

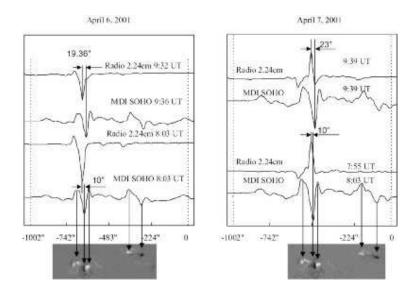
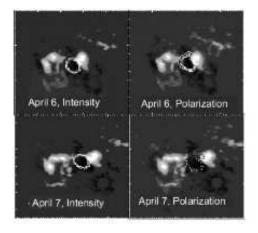


Figure 6: Comparison of 1D radio scans at wavelength 2.24cm and 1D MDI SOHO, for two time moments during April 6 and 7. This picture demonstrate the polarization inversion in radio with stable structure in optics.



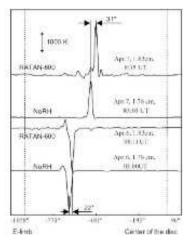


Figure 7: Comparison the radio data for two instruments Nobeyama radioheliograph at 1.7cm and RATAN-600 at 1.83cm for two days April 6 and 7. To the left- the comparison of 2D data. To the right- the comparison of 1D data with using convolution procedure. The radio data from two different telescopes confirm each other.

4.3 Polarization spectra during the period April 8-12 and their peculiarities

On the Figure 8 the spectral characteristics of AR during from April 4 till April 15, 2001 are compared with 2D maps from SSRT at 5.2cm. On the left spectra of intensity flux, on the center - spectra of the polarized emission (righthanded polarization points downwards) for the central intense radio source B are presented. On the right radio images at 5.2cm in intensity and circular polarization are shown. Here dotted contours correspond to the left-handed polarization, and solid line contours correspond to the righthanded one.

It is interesting to note, that a wide range polarization inversion which occurred from April 6 to 7 did not change the absolute character of a spectrum. The enhancement in a short-wave part of a spectrum preserved on April 7, although the sign of polarization turned to opposite (see Figure 8). The period from April 7 till April 11 was characterized by a steady growth of left polarization spectrum on short waves. This process lasted up to April 12 and was accompanied by intense X-ray flares, as seen on the Figure 3 and Table 1. Figure 8 demonstrates that SSRT registered the appearance of new

polarized source from the east side of the AR. Its intensity was monotonously rising and became dominant in the AR to the end of the period.

4.4 Features of polarization spectra during April 13 - 15

On April 12 - 13 the growth of a spectrum of the polarization flux on short waves has terminated. It is shown on the Figure 3, that flare activity on April 13 and 14 was considerably low. This reorganization has resulted in appearance of a new form of spectrum (Figure 9).

During this period on short wave range (1.83cm - 2.24cm) and on long waves (longer than 3.21cm) the sign of circular polarization has changed again to the righthanded. As seen on Figures 9 and 10, in a spectrum of polarized emission the intermediate frequency domain was formed, in which narrow (point) radio sources with numerous inversions of a circular polarization sign both on frequency and on time have appeared. In the paper [8] the domain was named as a "Frequency Domain of o- and e- Modes Coupling" (FDMC), because of multiple inversions of circular polarization on time and on frequency. Outside this frequency domain the polarization degree of the AR 9415 has decreased to small values (< 0.03%) (Figure 9), and in the channels of intensity (Figure 11) the "darkening effect" [22] has developed. As well as for a case with known Bastille day flare, this process has resulted in a powerful X14 flare at 13h 50m UT on April 15 (Figure 3).

5 Discussion

A variety of magnetic structures in solar AR atmosphere results in large variety of effects in microwave polarized emission, its variability on spectrum, on time, depending on flare activity etc.

It is well known, that the intensity and topology of coronal magnetic fields can influence the distribution and final polarization of radioemission from the underlying sources. The inversion of polarization sign occurs, when the emission on its way to the observer crosses a region, where the longitudinal component of an external magnetic field changes its direction: here the LH circular polarization of a radiosource becomes RH and vice versa. The inversion of polarization can also occur, if the radiation on different frequencies arises at different locations. As a result of different propagations through the

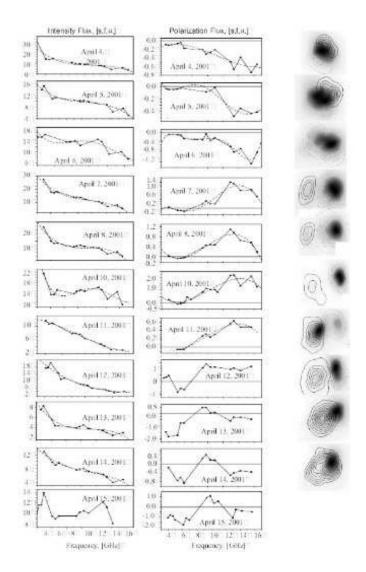
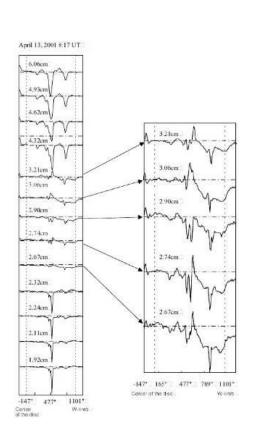


Figure 8: Comparison of RATAN-600 full flux spectra for intensity (to the left) and for circular polarization (in the centrum, to right- polarization is negative) with 2-D structure at 5.2cm. SSRT data are shown on the right column. Polarization maps (right polarization - solid line, left- dotted line) overlayed on intensity maps (the brightness is shown black color)).



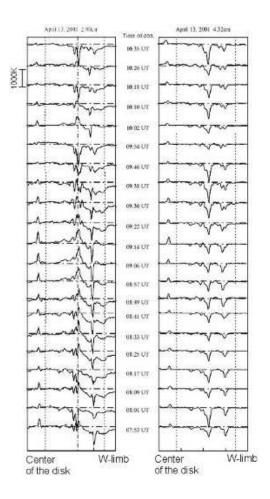


Figure 9: AR 9415 microwave emission polarization structure for April 13, 8:17UT. One can see the spectral peculiarity in the range 2.67cm - 3.2cm, where degree of polarization get weaker, the polarization structure sharply changing with wavelength. This is illustration of so named Frequency Domain of Modes Coupling (FDMC).

Figure 10: Evolution of AR 9415 polarization structure during April 13, from 7:53 UT to 10:35 UT. The wavelength 2.90cm is located inside the FDMC, and 4.32cm is outside the FDMC. Note multiple polarization inversions at 2.90cm on time. This phenomenon was registered in AR 9415 3 days before a big flare X14.4 on April 15, 13h50m UT.

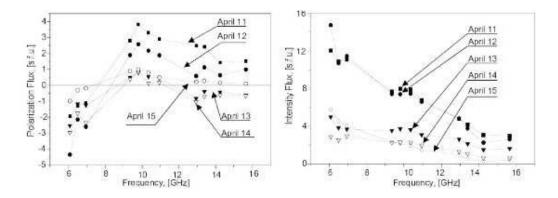


Figure 11: The "darkening" effect before the O14.0 flare at 13h 50m UT on April 15. To the right the intensity flux is decreased from day to day. To the left the polarization emission also is decreased with forming the band with weak polarization (FDMC)

area of inversion some parts of the source may undergo polarization inversion, while other parts do not show any polarization change.

Flare productive active regions demonstrate sharp changes of the sign and magnitude of polarization at the early preliminary phase of a flare as well as on its eruptive stage. It is widely accepted [3], that active processes on the Sun are obliged to the release of energy confined in magnetic fields. However, at the early preparatory phase of a powerful solar activity these processes take place on much smaller level of an energy-release. A question of places of localization of a primary energy-release [6] is not clear until now: where, at what heights, and how the primary energy-release is happening and the storage of energy in the magnetosphere of an active region occurs, which further results in the instability and realization of an active flare phase under the various possible scenarios [23]. It was unexpected the detection of fine structure of polarized radio emission spectra of flare productive active regions at early stages, several days prior to powerful flares [8]. It was shown, that such an initial heating occurs at low corona levels and can be registered with reflecting radio telescopes with high flux sensitivity in the range of 2cm - 5cm and detailed spectral - polarization analysis. Changes in a spectrum of polarized emission, inversions of polarization on frequency and on time, practically, always take place at the early stages of flare processes. The registered polarized emission from active region at this stage can reach very small values from several hundredth of s.f.u. up to several s.f.u. And

the degree of circular polarization can drop to some fractions of %. The analysis of the emission of the FPAR 9415 gives a number of new facts on evolution of active region, including several characteristic properties marked in a radio range. Detailed interpretation and modeling analysis will be stated in subsequent papers. Here we want to state the most probable versions of interpretation of the registered effects.

5.1 The rise of a new magnetic flux

The new magnetic flux rise is accompanied with an inversion and brightening of polarized emission in short wave part of centimetric range. The more probable hypothesis assumes the appearance of small islands of new rising magnetic flux with strength of 1500 - 2000 G and with sizes much smaller than the beam width θ_x θ_y at the level of low corona. This rising magnetic flux could be of a north or south polarity and could annihilate with an old (and more weak) magnetic flux with heterogeneous structure. Due to the high flux sensitivity of RATAN-600 (since a big effective area of antenna, high accuracy of polarization measurements, parallel multi wavelength analysis) a small islands of a new magnetic field can be registered at short wavelengths as a cyclotron emission. Let us make some estimations of sizes of rising magnetic flux islands for the case when the emission is fully polarized and it is determined by emission of extra-ordinary wave in the area of high coronal temperatures.

Taking into account the sensitivity in scan procedure with the fan beam of RATAN-600 at wavelength 2.24cm with beam sizes $\theta_x \theta_y = 17'' \times 15' = 15300''^2$ for an island with sizes $\theta_{xi} \cdot \theta_{yi}$ we can write:

$$\theta_{xi} \cdot \theta_{yi} = \frac{\theta_x \cdot \theta_y \cdot 2\sqrt{2} \cdot T_{n\odot}}{T_B \cdot \sqrt{\Delta f \cdot \tau}} \tag{1}$$

where $T_{n\odot}$ is a noise temperature of the system, including instrument noises T_n and quiet Sun antenna temperature $T_{\odot} = \alpha \cdot T_B$, approximately equaled 12000, where $\cdot T_B$ is brightness temperature of island, and $\alpha \simeq 2$.

With a bandwidth $\Delta f = 500 \mathrm{MHz}$, time constant $\tau = 0.2 sec$, we obtain a size of magnetic island $\theta_{xi} \cdot \theta_{yi} = 5''$ for temperature $T = 10^4 \mathrm{K}$, $\theta_{xi} \cdot \theta_{yi} = 0.5''$ for $T = 10^5 \mathrm{K}$ and $\theta_{xi} \cdot \theta_{yi} = 0.05''$ for $T = 10^6 \mathrm{K}$. Thus, high sensitivity is very important even for observations with moderate resolution of narrow and bright polarized details on the Sun.

In case of the polarity of new magnetic field coincides with the polarity of old magnetic field we register the rise of polarized flux at short wavelengths. In opposite case the short wavelength polarization inversion is observed. Thus from consideration for example of Figure 2, it follows that in the range of 1.92cm - 2.32cm we registered the rise of a new magnetic loop with a field strength of 1950 G at the base level and 1540 G at the top of the loop. The predominance of the extraordinary mode of emission on the 3-rd harmonic of gyrofrequency was assumed in these estimations.

The short wavelength brightening in spectrum of polarized emission of both signs was registered till April, 12 (Figure 2). This period was accompanied with strong flares (see Table 1, Figure 3 and 8) which argues for hypothesis of annihilation of a newly emerged magnetic flux with an old (and more weak) magnetic fields. Since the beam width of RATAN-600 at these wavelengths is approximately 17" × 15' and covers a significant area of active region it includes fine structured details of magnetic fields of both polarities. The convolution of the polarization beam of the radio telescope with an actual structure of radio brightness distribution is the difference of integrals over the right polarization and the left polarization. With assumption of cyclotron mechanisms of emission this convolution corresponds to the difference of magnetic fluxes at heights of radio emission of centimeter band. So, the observed structure of polarized emission is often complicated. The use of spectral-polarization analysis allow to separate the radio sources based on frequency spectra.

The discontinuance of short wavelength brightening in AR 9415 in period after April, 12 was accompanied with a cessation of activity and with preparation of a new scenario of flare energy release (see below for period of April 13 - 15).

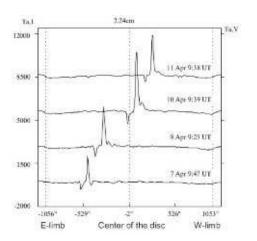
5.2 Recognized regularities of polarization inversion in AR 9415

In this Section we try to retrieve and analyze the spectra polarization changes originated strictly from the QT-propagation of microwaves through the solar corona on the way to observer.

5.2.1 Analysis of QT-propagation

Let us retrieve the well-known effects of QT-propagation from the challenging history of the spectra polarization changes in AR 9415 in the time period of April 3 - 15, 2000. For the sake of simplicity beginning with the AR 9415 at the central solar meridian on April 9, we will proceed to the limb positions. 3 microwave sources clearly seen at short cm wavelengths can be associated with the dominated sunspots of N-S-N magnetic polarity as A, B, and C sources of R-L-R sense of circular polarization correspondingly Figure 5.2.1. The above correspondence is evidenced by the RATAN-600 V scans Figure 6 (the LH circular polarization is positive and the RH is negative throughout the scans). It implies the prevalence of extraordinary mode radiation.

The AR persists as 2 microwave sources A and B of R-L sense of circular polarization in the SSRT maps (Figure 8) and in RATAN-600 scans at the wavelengths longer 5cm on April 7 - 11. The evolution of V scans at the long cm wavelengths clearly demonstrates the well-known regularities of polarization inversion [19]: the sense of polarization of the most limb ward source is inverted starting from the long wavelengths as the AR approaching either solar limb. Thus for the limb ward source B the first inversion started on April 12 at the wavelengths longer 6cm turning to the shorter wavelengths on April 13 (note R-R polarization structure at 5.2 on April 13; see Figure 8). The next (second) inversion in the source B occurred at the wavelengths longer than 6cm on April 14 - 15 (R-L structure). So far as a limb ward microwave source in western solar hemisphere is concerned. The source A (limb ward while in eastern hemisphere) is found to invert at the wavelengths longer than 6cm on April 5 - 6. The inversion turned to the wavelengths shorter than 5cm on April 6 - 7 (L-L structure). The next(second, if counting from the central meridian) inversion in the source A occurred closer to eastern limb on April 3 - 4, resulted in R-R polarization structure of the AR at the wavelengths shorter than 5.2cm. As for the longer wavelengths, the second inversion in the source A has completed up to April 3. The wavelengthdependent character of polarization inversion is illustrated by Alissandrakis [5] with the help of a QT-surface. The near-vertical QT-surface (where the propagation angle is equal to 90°) separates two opposite magnetic fluxes in an AR [4] and varies its inclination with the longitude. When the source is near the solar disk center, the microwaves ross QT-surface higher up in the corona, where the magnetic field is weak and the resulting polarization is the same as in front of the QT-surface. As the source moves towards the



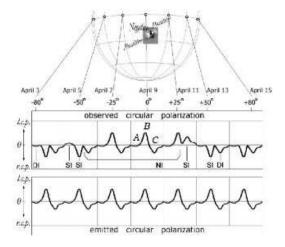


Figure 12: The AR 9415 polarization emission scans at wavelength 2.25cm made on RATAN=600 during April 7 - 11, 2001, which show R-L-R structure along solar longitude.

Figure 13: A sketch of polarization changes in the AR 9415 produced by two coronal regions of QT-propagation. The polarization inversions in 3 distinct microwave sources A, B, and C with longitudinal displacement from central meridian are illustrated by the evolution of V scan at 2.24cm. sources found to be of R-L-R sense of circular polarization while at the center of the solar disk. The A, B, and C sources are associated with N-S-N magnetic polarities of the underlying dominant sunspots. number of polarization inversions in a distinct microwave source within the "radio scan" is marked with SI for the singular inversion, with DI for the double inversion, and with NI for no inversion. Note that the polarization inversions appear in increasing number as the AR approaches the solar limb.

limb microwaves cross QT-surface lower in the corona, where the magnetic field is stronger and the sign of resulting circular polarization reverses at long wavelengths [25]. The closer an AR to solar limb is, the shorter is an operational wavelength required to detect the polarization inversion. At least two QT-surfaces are expected to separate N-S-N magnetic fluxes of the AR 9415. Thus, the source A has a chance to show the double polarization inversion while on the solar disk (Figure 5.2.1). During the first inversion, that is, on April 5 - 7 the AR photospheric fields are stable to the extent that the convolution with the RATAN-600 beam pattern looks like the radio scan in Stokes V at the short wavelength of 2.24cm (Figure 6). The stable (in a sense of polarity in the AR over the period of April 5 -12) photospheric magnetic fields give further evidence that the polarization radio inversion is caused by the propagation effects in the solar corona. In practice, the polarization inversion is easy observable and sure if the underlying microwave source is well resolved. Actually the limb ward microwave source was the first to invert the sense of polarization if watched from the solar disk center to either limb. It was the source A in the eastern hemisphere and C in the western. This source is found inverted twice at the longitudinal displacement of $50^{\circ} - 80^{\circ}$ from the central meridian, while the source closest to the meridian is found inverted once. The longitudinal asymmetry of the AR 9415 polarization inversions in two solar hemispheres results from the difference in the strength of the coronal fields in leading and following QTR. This difference is likely caused by both the different maximums of the photospheric fields and the dissimilar inclinations of the QT-surfaces admitted by [16] and [18]. It is worth noting the speedy completion of each polarization inversion in the NOAA 9415. Indeed, the only radio observation of April 6 succeeded to catch the moment of opposite signs of circular polarization within cm wavelength range in the course of the inversion. (There is no consideration to the complicated polarization effects of April 12 - 13.) Other observations with the RATAN-600 ([11], [20] have got records of both signs of polarization within cm wavelengths for the microwave source involved in the inversion. In the case of the AR 9415, all the inversions took much less than a day for completion in microwave range. We propose the steep gradients of the coronal magnetic fields in AR 9415 as the reason for the high speed and the abundance of the inversions.

5.2.2 Coronal magnetic field estimates

We can draw on the equation of the magnetic field B in QTR in relation to the transition wavelength λ to estimate the strengths of the coronal fields in the magnetosphere of AR 9415. The equation is derived from the parameter of the wave mode coupling in the QTR [25], provided the product of the electron density and the scale of the magnetic field divergence in the QTR is equal 10^{18} cm⁻² [7]:

$$B_{(G)} \simeq 180 \cdot \lambda_{\tau}^{-\frac{4}{3}}$$

As defined above, the transition wavelength is the wavelength of zero circular polarization as transition between two wavelengths ranges where opposite signs of circular polarization are to be observed. Closer examination of the AR 9415 at the eastern solar limb on April 3 (Figure 1) leads us to the conclusion that the microwave source A is risen to the height of $4 \cdot 10^9$ cm above the limb. Note that the near-limb polarization inversion in the source A occurs at $\lambda = 2.5$ cm (transition frequency equals to 12 GHz; see Figure 1). This requires as strong coronal fields as 53 G to produce the observed inversion in the QTR at the height no less than the height of the source $(h > 4 \cdot 10^9 \text{cm})$. The microwave sources B and C seem to be overlapped and polarized in RH sense. On the evidence of the polarization inversion in the source B at $\lambda = 5$ cm on April 6 (Figure 8) one can estimate the coronal field to be 21 G in the QTR covering the source B. The most effective determinations of the relevant QTR heights imply the detailed model analysis [7]. The rough estimates can be made by the rate of polarization inversion [11]. For April 6 observations of the source B (31" in diameter; 1 day interval taken for polarization inversion; $\lambda = 5 \text{cm}$) this method yields a height of $6 \cdot 10^9 \text{cm}$ for the coronal field of 21 G.

5.3 The effects of darkening and formation frequency domain of modes coupling

The active region 9415 went on to the new state starting from 13th of April. From the one hand, this state is characterized by appearance of the an intermediate frequency domain of o- and e- Modes Coupling" (FDMC) with low polarization signal and multiple inversions of polarization, from the other hand, the effects of darkening emission in intensity channels were observed (Figure 11).

The similar phenomenon was observed before the Bastille day flare at April 14, 2000 [22]. Here we considerate this phenomenon in detail due to the frequent multiazimuth observations. On the Figure 9 the multi-frequency scans of AR9415 are presented for one azimuth. On the right the FDMC of this AR is shown on the big scale. One can see that the signal inside of FDMC band is significantly smaller then out of it. And at the same time the polarization structure in the band of 2.67cm - 3.21cm is changed abruptly from one wavelength to another (Figure 9). We have compared the activity inside of FDMC band at wavelength 2.90cm and outside of this band at 4.32cm. It is seen that in this AR the leap forward processes (probably nonthermal) at wavelength 2.90cm were occurred continuously from 7:53 UT to 10:35 UT (see the AR in the middle of the left on the Figure 10)). On the right the temporal behavior of this AR at wavelength 4.32cm during the same interval of time is shown. One can note there is not any polarization inversion in the AR, but the corresponded variations of the polarization emission are presented. This phenomenon was being exist 3 days until the moment of X14 flare at 13:50 UT on April 15.

The spectra of intensity and circular polarization for five days before the flare are presented on the Figure 11. In the intensity channels the effect of darkening became apparent rather clearly from day to day, and the gradual formation of FDMS band can be traced in the polarization channels. The interpretation of this phenomenon was proposed in paper [22] as the propagation of cyclotron radio emission through the cold filament based on the model [24]. However, this model does not explain both the abrupt changes of polarization structures from wave to wave and the temporal changes (see Figures 9 and 10). Thus, the analysis of AR 9415 observations revealed the diversity of polarization characteristics taking place during early preparatory stage, during the pre-erupting stage and the main stage of a strong flare.

6 Conclusions

The comprehensive investigation of the flare productive active region NOAA AR 9415 have revealed that polarized emission in broad range of wavelengths represent a complicated structure of the active region's magnetosphere. The presence of multiple polarization inversions could be caused both by a flare productive nature of the active region and as well as the geometry of propagation of microwaves through quasi transverse magnetic fields. To evaluate

correctly the magnetic field parameters in broad range of coronal heights from 1000 km to some 100000 km it is necessary to perform a spectral analysis of the emission in a broad wavelength range in combination with two-dimensional mapping at single waves and with satellite data on optical and X-ray bands. In the paper for the first time the complete evolution of QT-effect over a full time of the AR passage along the solar disk was studied at several wavelengths in simultaneous observations.

The polarization inversion is intrinsical feature of flare-productive active region on the preparatory, pre-eruptive and eruptive stages. This inversion and other effects (such as multiple polarization inversions on frequency and on time, the effect of microwave darkening before a strong flare, short wave polarization increasing etc) are sharply revealed both in circular polarization emission spectrum and its temporal changes. The new polarized emission phenomenon discovered require adequate model investigation and appropriate observations with high parameters in sensitivity, space and temporal resolution. The high sensitivity of radio waves to magnetic fields could be used for understanding of active processes going on at different heights of the solar atmosphere.

7 Acknowledgments

The authors thank INTAS (grant 0181 and 0543) which allowed to join the efforts of different scientific groups in this work.

References

- [1] Alissandrakis, C.E. and Preka-Papadema, P.: 1984, Astron. Astrophys., 139, 507.
- [2] Alissandrakis, C.E., Nindos, A., Kundu, M.R.: 1993, Solar Phys., 147, 343.
- [3] Alissandrakis K.E.: "Magnetic field of the Solar Corona", in Advances in Solar Phycics, ed. by G.Belvedere, M. Rodono, G.M.Simnett (Springer, 1994), 432, 109.
- [4] Alissandrakis, C.E., Borgioli, F., Chiuderi Drago, F., Hagyard, M., Shibasaki, K.: 1996, Solar Phys., 167, 167.

- [5] Alissandrakis, C.E.: 1999, Proc. of Nobeyama Symp., NRO Report 479, 53.
- [6] Bastian T.S., Benz A.O., Gary D.E.: 1996, Ann.Rev.Astron.Astrophys. 36, 131.
- [7] Bezrukov, D.A., Grechnev, V.V., Ryabov, B.I.: 2003, Baltic Astronomy, (submitted).
- [8] Bogod, V.M., Tokhchukova, S.Kh. 2003, Astronomy Letters, 2003, 263.
- [9] Bogod V.M., Zhekanis G.N., Mingaliev M.G., Tokhchukova S.Kh: 2003, Izvestiya vuzov, Radiofisika (submitted, in Russian)
- [10] Bogod, V.M., Kotelnikov V.S., Yasnov L.V.: 2003, Astron. Rep., submitted.
- [11] Gelfreikh, G.B., Peterova, N.G., Ryabov, B.I.: 1987, Solar Phys., 108, 89.
- [12] Cohen R.,1960,ApJ. 131, 664.
- [13] Gelfreikh, G.B., Pileyva, N., and Ryabov, B.I.: 1997, Solar Phys., 170, 253.
- [14] Gopalswamy, N., Zheleznyakov, V.V., White, S.M., and Kundu, M.R.: 1994, Solar Phys., 155, 339
- [15] Kaltman T.I., Korzhavin A.N.: 2003, Astron. Rep. (submitted)
- [16] Kundu, M.R. and Alissandrakis, C.E.: 1984, Solar Phys., 94, 249.
- [17] Maksimov, V.P. and Bakunina, I.A.: 1991, Sov. Astron., 35, 194.
- [18] Lee, J., White, S.M., Kundu, M.R., Mikic, Z., McClymont, A.N.: 1998, Solar Phys., 180, 193.
- [19] Peterova, N.G., Akhmedov, Sh.B.: 1974, Soviet Astron., 17, 768.
- [20] Ryabov, B.I., Pilyeva, N.A., Alissandrakis, C.E., Shibasaki, K., Bogod, V.M., Garaimov, V.I., Gelfreikh, G.B.: 1999, Solar Phys., 185, 157.

- [21] Ryabov, B.I., Maksimov, V.P., Lesovoi, S.V., Shibasaki, K., Nindos, A., Pevtsov, A.A.: 1999, Solar Phys., (submitted).
- [22] Tokhchukova S.Kh., Bogod V.M.: 2003, Solar Phys., 212/1, 99
- [23] Vrsnak, B.:2003, in "Energy Conversion and Particle Acceleration in the Solar Corona", ed. by K.L.Klein, 28.
- [24] Zlotnik E.Ya.: 2001, Radiophysics and Quantum Electronics, 44/1-2, 53.
- [25] Zheleznyakov, V.V.: 1970, Radio Emission of the Sun and Planets, Oxford, Pergamon Press.